ModEst - Precise estimation of genome size from NGS data

Markus Pfenninger[1,2,3], Philipp Schönnenbeck[3], Tilman Schell[2]

[1] Senckenberg Biodiversity and Climate Research Centre, Georg-Voigt-Str. 14-16, 60325 Frankfurt am Main, Germany

[2] LOEWE Centre for Translational Biodiversity Genomics, Senckenberg Biodiversity and Climate Research Centre, Frankfurt am Main, Germany

[3] Institute for Organismic and Molecular Evolution, Johannes Gutenberg University, Mainz, Germany

Corresponding author: Markus Pfenninger (Markus.Pfenninger@senckenberg.de)

Abstract

Precise estimates of genome sizes are important parameters for both theoretical and practical biodiversity genomics. We present here a fast, easy-to-implement and precise method to estimate genome size from the number of bases sequenced and the mean sequence coverage. To estimate the latter, we take advantage of the fact that a precise estimation of the Poisson distribution parameter lambda is possible from truncated data, restricted to the part of the coverage distribution representing the true underlying distribution. With simulations we could show that reasonable genome size estimates can be gained even from low-coverage (10X), highly discontinuous genome drafts. Comparison of estimates from a wide range of taxa and sequencing strategies with flow-cytometry estimates of the same individuals showed a very good fit and suggested that both methods yield comparable, interchangeable results.

Introduction

Eukaryotic genomes vary tremendously in size (Oliver *et al.* 2007; Bennett & Leitch 2005; Petrov 2001; Kapusta *et al.* 2017; Carta *et al.* 2020), yet the underlying processes for this variability are not yet fully understood (Elliott & Gregory 2015). To understand and study mechanisms of genome size variation, such as proliferation of repetitive elements (Blommaert *et al.* 2019), effective population size (Lefébure *et al.* 2017; Lynch & Conery 2003) or correlation to other traits (Gardner *et al.* 2020; Prokopowich *et al.* 2003), reliable estimates for the taxon under scrutiny are therefore mandatory. This is all the more important as substantial changes in genome size may even occur among closely related sister species, i.e. over relatively short evolutionary time scales (Keyl 1965; Agudo *et al.* 2019, Vitales et al. 2020). A precise estimation of genome size is also important for genomic projects. For example, in the assembly of genomes, the proportion of the true genome size covered by a given assembly draft is a quality criterion and limits the maximum size of the draft. Also resequencing

projects requiring a certain coverage e.g. for genotyping profit from a reliable genome size estimate (Fountain *et al.* 2016).

Flow cytometry is generally deemed to yield reliable estimates of genome size (Johnston *et al.* 2019; Doležel & Greilhuber 2010). Yet, this method is not without caveats (Wang *et al.* 2015) and requires specialised laboratory skills and availability of the relatively expensive equipment. Moreover, the method depends on availability of fresh or frozen tissue with largely intact cells, which narrows the range of taxa for which such analyses are practically feasible (Johnston *et al.* 2019).

Bioinformatical analysis of next generation sequencing data provides an alternative for estimating genome size (Vurture *et al.* 2017). Besides the widely used k-mer based methods (Lipovský *et al.* 2017; Li & Waterman 2003), Schell et al. 2017 introduced a very simple method for genome size estimation, relying on mapping statistics of NGS reads mapped back to a draft assembly. The approach assumes that the probability to sequence a genome position is identical over the entire genome, i.e. that their true coverage is Poisson distributed. Even though there is a slight bias regarding the double strand breaking positions during DNA preparation for NGS sequencing, the impact on the resulting sequencing coverage distribution is negligible (Poptsova et al. 2014). In a perfect assembly covering the entire genome, lambda as the parameter of the underlying Poisson distribution (as well as the mean and median) of the coverage distribution should therefore be identical to the true coverage. Dividing the number of sequenced, successfully back-mapped bases by the lambda of the observed coverage should yield a precise estimate of the true genome size. In most real draft genomes, however, repetitive regions are not resolved which results in collapsed repeat regions, and in an assembly that is shorter than the true length (Treangen & Salzberg 2012). These collapsed repeat regions are over-proportionally covered, skewing the coverage distribution, and hence, estimates of lambda upwards. A second source of systematic error in assemblies are relatively diverged heterozygous regions, e.g. from inversions that are not identified as homologous. These will result in a double representation of the respective region in the genome, making it longer (Asalone *et al.* 2020). Consequently, the expected coverage of these regions in the assembly will be half of the true coverage and skew the coverage distribution and parameters estimated from it downwards. In real genome assemblies, both errors likely occur to various extents (Sohn & Nam 2018), rendering a naïve use of parameters estimated from the observed coverage distribution misleading.

We show here how the observed coverage distribution and an estimate of the number of bases sequenced from genome assembly drafts can be used to infer precise estimates of genome size. We name the approach ModEst from **Mod**al **Est**imation of genome size. We tested the methods with simulations, including various degrees of divergent heterozygous sites and a tetrapoid genome, and

66 compare genome size estimates from real data over a wide range of genome sizes with those derived
67 from flow cytometry and k-mer based methods.

68 Material and Methods

69 *Theoretical background*

70 Under the assumption that NGS sequencing methods sequence all bases in a genome with equal
71 probability, dividing the number of bases sequenced (N) by the true length of the genome (L) yields
72 the mean or expected coverage (c) (Sims *et al.* 2014).

73 $$c = N / L$$

74 Since the coverage distribution is discrete, it can be modelled by a Poisson distribution with
75 parameter λ as c. As we are interested in L, we need to find reliable estimates for N and c from
76 empirical data.

77 The number of bases used for the assembly of a particular genome is usually known. This number is,
78 however, not necessarily identical to the number of bases sequenced from the target genome.
79 Depending on the origin of the DNA, the data set may contain more or less reads originating from
80 contaminations, the microbiome, and certainly reads from the mitochondrial or plastid genomes
81 (Kumar *et al.* 2013). Even though several tools and pipelines exist to remove the bulk of such reads
82 (Chaliis et al. 2020), this rarely succeeds completely. The number of bases after thorough cleaning,
83 N_{clean}, estimates therefore rather the upper limit of N.

84 An alternative is the number of bases mapped back to the genome assembly draft N_{bm}. For this
85 number to represent a good approximation of the number of bases sequenced from the
86 corresponding genome, all genomic elements (telomers, centromers, repeats) must be represented
87 in the assembly at least once without presence of contamination etc. and all reads must map back.
88 This number is therefore a lower limit estimator of N.

89 As detailed in the introduction, the empirical coverage distribution of back-mapped reads is usually
90 biased by errors in the genome draft due to collapsed repeats and/or other assembly errors.
91 However, commonly at least a substantial part of the back-mapped reads map to unique sequences
92 in the genome draft and should consequently show a coverage distribution following the true
93 underlying Poisson distribution. Estimating λ from the part of the distribution we know is not biased
94 by assembly errors should therefore yield a reliable estimator of c. In Schell et al. 2017, the modal
95 value of the empirical coverage distribution (m), i.e. the most often observed coverage was used as
96 an estimator of c. The modal value is a fairly good approximation of λ because the difference is in all
97 cases smaller than or equal to 1 and therefore becomes relatively less biased when λ is high (i.e. high

mean coverage). Nevertheless, better methods for estimating λ from truncated Poisson distributions exist (Delignette-Muller & Dutang 2015; Nadarajah & Kotz 2006; Böhning & Schön 2005; David & Johnson 1952).

As mentioned above, the coverage distribution may show more than a single peak. One possibility to obtain a bimodal distribution arises from highly divergent heterozygous tracts in the respective genome. In the assembly process, such divergent tracts may not be identified as homologous by the algorithm and thus occur as separate regions. Consequently, the coverage in such areas is only half the true coverage. If a considerable proportion of the genome consists of such divergent heterozygous regions, a second peak may appear in the coverage histogram. It has its maximum usually at half the coverage of the larger peak. In this case, the peak with the larger coverage represents the true coverage. Except for recent hybrid individuals, the latter peak should nevertheless always be the higher one.

Another possibility to obtain a multimodal coverage distribution arises from polypoid species. If the multiplied genomes diverged to an extent that both are completely represented in the assembly, the genome size estimation process is not any different from a diploid species. The other extreme would be a multiplied genome that is so little diverged that only a single copy appears in the assembly. In an intermediate stage, some more diverged parts of the multiplied genomes may be resolved, while others are collapsed in the assembly. The collapsed parts are expected to be over-covered and therefore the lowest peak represents the true coverage.

In general, the observation of a multimodal coverage distribution of the backmapped reads is indicative of issues with the assembly. Genome size estimation with the proposed ModEst method should be nevertheless possible, given appropriate caution.

Practical approach

All the figures needed to estimate the genome size according to the method described here are usually collected in the process of genome assembly or can be easily calculated with standard tools. In particular, samtools stats and bedtools genomecov can be used for this purpose. The output of samtools stats provides information on bases sequenced and mapped, while the output of bedtools genomecov provides the empirical coverage distribution. The latter can be used as input for R. After preparing the data, we first estimated the modal value of the empirical distribution. This modal value is used as starting point for a Maximum Likelihood method to estimate λ from a truncated Poisson distribution as implemented in the R-libraries *truncdist* and *fitdistrplus* (Delignette-Muller & Dutang 2015; Nadarajah & Kotz 2006). We empirically determined suitable upper and lower truncation limits and give recommendations below. The respective R-code can be found in the Supplement and a Perl

131 wrapper-script, including all necessary dependencies can be found at
132 https://github.com/schellt/backmap.

133 *Simulations*

134 To illustrate the influence of factors like sequencing depth, genome size, repeat content and -
135 distribution on the different genome size estimation methods, we simulated five different genomes
136 according to real examples. Publicly available genome assemblies and annotations of *Saccharomyces*
137 *cerevisae*, *Caenorhabditis elegans*, *Arabidopsis thaliana*, *Drosophila melanogaster* and *Scophthalmus*
138 *maximus* were used to obtain distributions of size and distance between annotated repeat regions.
139 Simulated genomes of the size of the five genome assemblies mentioned above were then created
140 using a custom Python-tool, available at https://github.com/Croxa/Simulate-Genome. Regions
141 annotated as repeat regions (rr) were filled with random repeat units up to 10 bp length, high
142 complexity regions with random nucleotides. For sake of ease, we simulated the genomes on a single
143 chromosome. A mean GC content of 0.5 was applied to both categories. Characteristics of the
144 simulated genomes can be found in Table 1.

145 Table 1: Simulated genomes and their characteristics, rr = repeat regions.

Simulated genome	Size (Mbp)	average count of bases between rr	average count of bases of rr	% of rr
1 *Saccharomyces cerevisae*-like	12	1246.68	156.67	5.26
2 *Caenorhabditis elegans*-like	100	508.66	166.42	13.23
3 *Arabidopsis thaliana*-like	120	622.32	311.55	18.06
4 *Drosophila melanogaster*-like	144	372.42	242.48	23.39
5 *Scophthalmus maximus*-like	524	521.84	45.64	3.74

146

147 From these simulated genomes, we generated synthetic next-generation sequencing short read sets
148 of 10X, 30X and 60X coverage using ART Illumina 2.5.8 (Huang *et al.* 2012). This tool emulates the
149 sequencing process with built-in, technology-specific read error models, base quality value profiles
150 parameterized empirically for large sequencing datasets and even adds the sequencing adapters. The
151 reads were simulated paired-end, length of 150 bp with a standard deviation of 10 and an insert size
152 of 300 bp. The Illumina sequencing system profile was HiSeq 2500 (HS25).

153 The read sets were trimmed with Trimmomatic 0.39 (Bolger *et al.* 2014). Trimmed were usual
154 Illumina adapters (ILLUMINACLIP:adapter.fa:2:30:10), leading and trailing bases with a quality score

155 lower than 5, sliding windows with the size of 20 and an average quality score below 5 and reads
156 with a length of 50 or lower.

157 In a first set of experiments, the trimmed read sets of different coverage were back-mapped to the
158 simulated genomes they were derived from. Mapping was executed within the wrapper script
159 backmap.pl using bwa mem 0.7.17 without changing default options from backmap.pl. BWA
160 (Burrows-Wheeler Aligner) is a widely used algorithm for mapping low-divergent sequences against a
161 large reference genome (Li 2013).

162 To estimate the influence of genome assemblies of varying quality on the accuracy of the genome
163 size estimate, we assembled each read set with SPAdes, the St. Petersburg genome assembler. This
164 algorithm is implemented in a toolkit containing various assembly pipelines (Bankevich *et al.* 2012).
165 SPAdes 3.13.0 was used to assemble both trimmed paired and unpaired reads in a one-pass assembly
166 using default options. The respective read sets were back-mapped and analysed as described above.
167 For one simulation (*A. thaliana*-like, 10X coverage), we evaluated the effect of different truncation
168 limits on the precision of the λ estimation. For coverage class windows ranging from 11 to 5, centred
169 on the modal value, the deviation of the ML estimate decreased from 0.4% to 4%. We performed the
170 λ calculations therefore with a window size of eleven around the estimated modal value.

171 The influence of different amounts of diverged heterozygous genome stretches on size estimation
172 was evaluated using the Saccharomyces-like genome. We simulated the genome with X,Y and Z%
173 heterozygous stretches. To make sure that these stretches were not collapsed in the assembly
174 process, we chose a sequence divergence of 10%. Likewise, we inferred the effect of polyploidy on
175 genome size estimation with our method. We doubled the Saccharomyces-like genome and
176 randomly changed bases in the complex part of one of the genomes. We simulated divergences of
177 0.5%, 1% and 5% among the two genomes. Both sets of simulations were performed as described
178 above with 30X coverage.

179 For all simulations, we calculated four different genome size estimates:

180 i) N_{clean}/λ, the number of "sequenced" bases after cleaning and trimming divided by the
181 truncated Poisson ML λ estimate derived from the empirical coverage distribution.
182 ii) N_{clean}/m, the number of "sequenced" bases after cleaning and trimming divided by the
183 modal value of the empirical coverage distribution.
184 iii) N_{bm}/λ, the number of back-mapped bases divided by the ML λ estimate derived from the
185 empirical coverage distribution.
186 iv) N_{bm}/m, the number of back-mapped bases divided by the modal value of the empirical
187 coverage distribution.

188 For each estimate, we calculated the relative deviation from the true known genome size.

189 *Empirical data*

190 We used data from de novo genome assemblies that were sequenced in the last few years at the
191 LOEWE Translational Biodiversity Genomics Centre and for which flow cytometry estimates from the
192 same individual/clone/population were available. The taxonomic range of genomes comprised plants
193 and several animal taxa with a focus on insects (Table 2).

194 Table 2. Genomes used for empirical evaluation.

Species	Taxon	Flow-cytometry estimate [Mb]	Backmapping estimate [Mb]	k-mer based estimate [Mb]	Sequencing technique	Citation
Hydropsyche tenuis	Insecta	260.6	228.6	222.8	Short read	Heckenhauer *et al.* 2019
Plectrocnemia conspersa	Insecta	455.2	364.9	316.3	Short read	Heckenhauer *et al.* 2019
Agapetus fuscipens	Insecta	721.8	583.5	463.2	Short read	Heckenhauer et al. 2021
Odontocerum albicorne	Insecta	1616.0	1270.0	1103.4	Short read	Heckenhauer et al. 2021
Drusus annulatus	Insecta	840.2	684.3	592.3	Short read	Heckenhauer et al. 2021
Halesus radiatus	Insecta	1212.4	972.3	918.7	Short read	Heckenhauer et al. 2021
Micropterna sequax	Insecta	1434.7	1100.0	981.7	Short read	Heckenhauer et al. 2021
Micrasema longulum ML1	Insecta	663.6	707.7	650.7	Short read	Heckenhauer et al. 2021
Micrasema longulum ML3	Insecta	663.6	637.8	635.2	Short read	Heckenhauer et al. 2021
Micrasema minimum	Insecta	588.8	329.3	333.8	Short read	Heckenhauer et al. 2021
Rhyacophila evoluta Rss1	Insecta	651.3	581.8	518.8	Short read	Heckenhauer et al. 2021
Rhyacophila evoluta HR1	Insecta	651.3	565.5	514.4	Short read	Heckenhauer et al. 2021
*Glaux maritima (*also known as *Lysimachia maritima)*	Angiosperm plant	1270.0	1541.4	1221.3	Short read	Segers et al. unpublished data

Radix auricularia	Mollusca	1575.0	1603.0	947.1	Short read	Schell *et al.* 2017
Crematogastor levior	Insecta	455.0	356.0	255.9	Short read	Hartke *et al.* 2019
Daphnia galeata	Crustacaea	155.0	157.0	150.5	Short read	Nickel *et al.* 2021
Candidula unifasciata	Mollusca	1540.0	1420.0	977.6	Short read	Chueca *et al.* 2021a
Styela plicata	Tunicata	430.9	468.6	338.8	Short read	Galià-Camps et al. unpublished data
Callionymus lyra	Teleostei	645.0	653.2	562.0	Short read	Winter *et al.* 2020
Pimpla turbinella	Insecta	300.0	298.0	206.0	Short read	Reumont et al. unpublished data
Fagus sylvatica	Angiosperm plant	582.4	542.0	541.0	Short read	Mishra *et al.* 2021
Aedes japonicus	Insecta	857.0	836.3	699.0	Short read	Reuss et al. unpublished data
Nyctereutes procynoides	Mammalia	3100.0	3230.0	-	Long read	Chueca *et al.* 2021b
Microthlaspi erraticum	Angiosperm plant	194.5	211.0	211.00 -	Short read	Mishra *et al.* 2020
Crematogastor levior, species B	Insecta	390.0	406.7	-	Long read	Feldmeyer et al. unpublished data
Camponotus femoratus	Insecta	330.0	340.0	-	Long read	Feldmeyer et al. unpublished data
Astacus astacus	Crustacaea	16891.0	16750.0	-	Short read	Theissinger et al. unpublished data
Lamprophis fuliginosis	Squamata	1480.0	1617.0	-	Long read	Hiller et al. unpublished data
Desmodus	Mammalia	2337	2089	-	Long read	Hiller et al. unpublished data

If not stated otherwise in the citations, genome size estimates from flow cytometry were estimated following a protocol with propidium iodide-stained nuclei described in (Hare & Johnston 2012). Tissue of the organism was chopped with a razor blade in a petri dish containing 2 ml of ice-cold Galbraith buffer. The suspension was filtered through a 42-µm nylon mesh and stained with the intercalating fluorochrome propidium iodide (PI, Thermo Fisher Scientific) and treated with RNase II A (Sigma-Aldrich), each with a final concentration of 25 µg/ml. The mean red PI fluorescence signal of stained nuclei was quantified using a Beckman-Coulter CytoFLEX flow cytometer with a solid-state laser emitting at 488 nm. Fluorescence intensities of 5000 nuclei per sample were recorded. We used the software CytExpert 2.3 for histogram analyses The total quantity of DNA in the sample was calculated as the ratio of the mean red fluorescence signal of the 2C peak of the stained nuclei of the target organism divided by the mean fluorescence signal of the 2C peak of the reference standard times the 1C amount of DNA in the standard reference. Six replicates were measured on six different

208 days to minimize possible random instrumental errors. We report the mean value of these
209 measurements.

210 For each of the genomes, we calculated N_{bm}/m since we could not reconstruct the exact state of
211 taxonomic read cleaning i.e. removal of contamination reads from other taxa for all genomes. The
212 modal value was chosen, because the coverage exceeded 50X in most cases. For comparison, we
213 performed or used published k-mer based estimates as far as available. First a k-mer profile was
214 generated from Illumina reads using jellyfish 2.3.0 tools (Marçais & Kingsford 2011) count with a
215 length of *k*=21 and counting k-mers on both strands and histo. Subsequently, the generation
216 histogram was used as input for the GenomeScope webserver (Vurture *et al.* 2017) together with the
217 above mentioned length of k and read length. For some organisms, the approach could find no
218 appropriate model. In addition, it is not suitable for long read technologies.

219 *Statistical analysis*

220 The performance of the two bioinformatic genome size estimation methods was evaluated by their
221 linear regression fit with the respective flow-cytometry estimates. We compared the two slopes of
222 the regression for statistical difference (Cohen *et al.* 2013).

223 Results

224 *Simulations*

225 The single-pass assemblies derived from the simulated short reads were highly fragmented with
226 thousands of short scaffolds, almost independent of simulated coverage (Table 3). For the
227 *S. saccharomyces*-like, the *C. elegans*-like and the *S. maximus*-like genomes, the total lengths of the
228 assemblies were above 90% of the true size, for the remaining two below 80%. This was reflected in
229 the back-mapping rates that were highly correlated to the relative assembly length ($r = 0.995$, $p <$
230 0.001, Table 3).

231 Table 3. Characteristics of simulated genomes, their assemblies, back-mapping and estimation of the parameter of the underlying Poisson-distribution.

232

Simulated genome	simulated coverage	true size [Mbp]	assembly size [Mbp]	proportion of true length	number of contigs	mean contig length [bp]	Mbp "sequenced" $=N_{clean}$	bp mapped $= N_m$	proportion of bases mapped
*Saccharomyces_cerevisae*_like	10	12.08	11.24	0.930	2,021	5,561	120.8	113.0	0.931
	30	12.08	11.24	0.931	1,823	6,170	362.4	339.1	0.932
	60	12.08	11.24	0.932	1,906	5,905	724.8E+08	677.7	0.931
*Caenorhabditis_elegans*_like	10	100.0	92.77	0.927	105,104	883	100.0E+09	933.7	0.904
	30	100.0	9280	0.928	98,341	944	300.1E+09	2807	0.910
	60	100.0	92.25	0.929	99,957	930	600.2E+09	5598	0.904
*Arabidopsis_thaliana*_like	10	120.1	92.83	0.773	66,881	1,388	1201	956.6	0.780
	30	120.1	93.03	0.775	63,695	1,461	3602	2881	0.785
	60	120.1	92.75	0.772	61,615	1,505	7205	5759	0.784
*Drosophila_melanogaster*_like	10	144.1	107.8	0.748	104,002	1,037	1441	1118	0.755
	30	144.1	107.7	0.747	95,701	1,125	4322	3382	0.763
	60	144.1	107.6	0.747	95,523	1,127	8643	6725	0.756
*Scophthalmus_maximus*_like	10	524.1	523.4	0.999	76,507	6,842	5241	5220	0.994
	30	524.1	524.1	1.000	63,360	8,261	15720	15670	0.995
	60	524.1	425.1	1.000	63,260	8,274	31440	31340	0.995
*Saccharomyces_cerevisae*_like 1% divergent heterozygous regions	30	12.08	11.78	0.975	1,152	10,226	356.1	352.2	0,989
5% divergent heterozygous regions	30	12.08	12.18	1.008	3,020	4,032	354.0	350.5	0,990
10% divergent heterozygous regions	30	12.08	12.68	1.049	5,435	2,333	351.4	347.1	0,988
10% divergent heterozygous regions	30	12.08	13.68	1.133	10,163	1,346	346.1	341.9	0,988
Tetraploid Saccharomyces_cerevisae_like 0.5% divergence among duplicated genomes	30	24.16	11.75	0.486	1,197	9,818	712.9	700.4	0.982
1% divergence	30	24.16	13.09	0.542	6,699	1,954	713.0	696.8	0.977
5% divergence	30	24.16	22.92	0.949	4,719	4,857	714.4	700.3	0.980

233

234 The least relative deviation from the true genome size overall was found for the N_{clean}/λ estimator
235 (mean deviation 0.00017, range 0.00003-0.00056), followed by N_{clean}/m (0.054, 0.0169 - 0.111),
236 N_{bm}/m (0.094, 0.014-0.209) and N_{bm}/λ (0.112, 0.003-0.224, Figure 1). There was a tendency for the
237 method to perform better with higher coverage, mainly due to the smaller relative deviation of *m*
238 from λ at higher coverage. Given the rather minor differences in contiguity among genome
239 assemblies reconstructed from different coverages, this factor had only a minor role for the precision
240 of the genomes size estimates (Table 3, Figure 1).

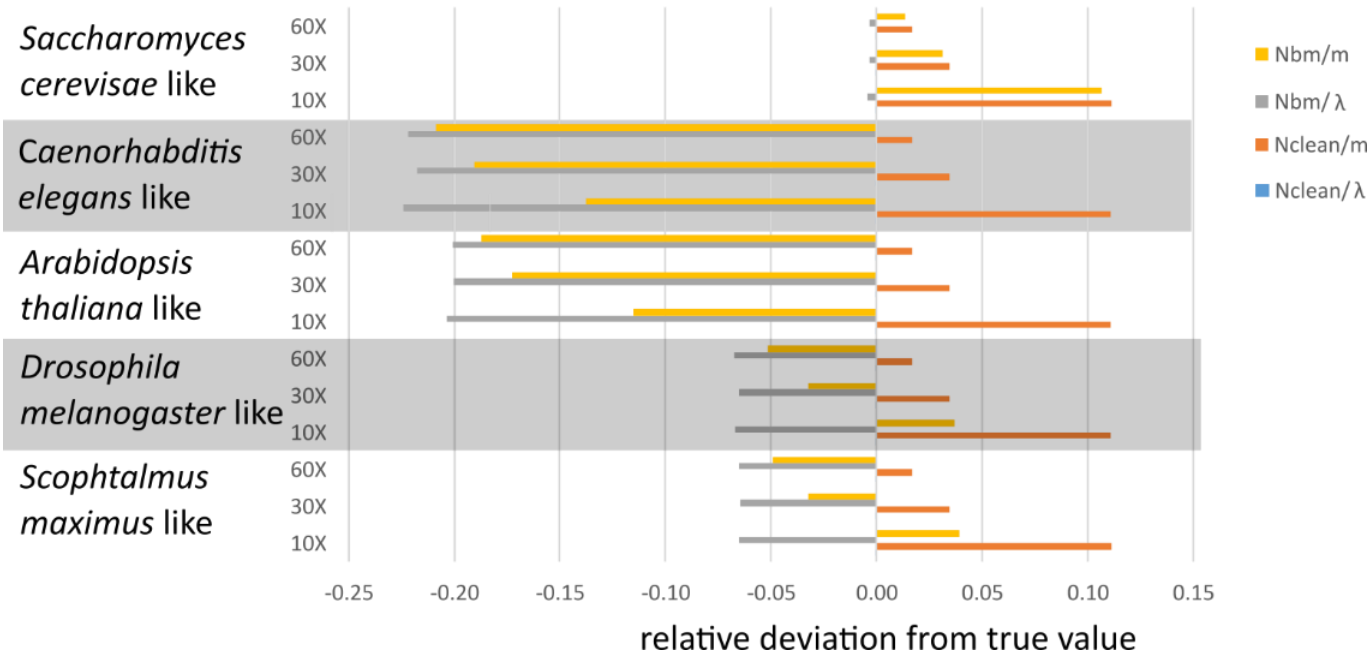

241

242 Figure 1. Relative deviations of genome size estimators from true values for different simulated
243 genomes and simulated coverages. The deviations of N_{clean}/λ (blue) from the true value are so small
244 that they are not visible on the scale. The raw data table to this figure can be found in the
245 Supplemental Table 1.

246 The genome size estimates from simulated genomes with varying proportions of divergent
247 heterozygous sites all yielded the same estimates (Supplemental Table 1). As can be seen in the
248 respective coverage distributions, the only difference between the simulations was a second, lower
249 peak at about half the expected coverage that grew with increasing amount of heterozygous regions.
250 The position of the true peak remained unaffected (Figure 3a).

251 Assembly of a tetraploid *Saccharomyces cerevisae*-like genome with the two lowest divergences
252 between the duplicated genomes (0.5% and 1%) resulted in the reconstruction of approximately a
253 single haploid genome, respectively (assemblies of lengths 1.18 Mb and 1.31 Mb, Supplemental
254 Table 1). Therefore, the highest observed coverages for these simulations were both 59 and the λ
255 estimates close to 60 (Supplemental Table 1, Figure 3b). Consequently, the genome size estimates

256 were close to the haploid length. However, with divergence 1%, a second peak with maximum 28,
257 respectively λ 28.9 emerged (Figure 3b, Supplemental Table 1). Using this peak yielded estimates that
258 were much closer to the truth (relative deviations between 0.005 and 0.06, depending on estimator).
259 With 5% divergence, the duplicated genomes were almost fully resolved in the assembly and, hence,
260 the peak at the true coverage and therefore the genome size estimates not further than 0.03 from
261 the truth (Figure 3b, Supplemental Table 1).

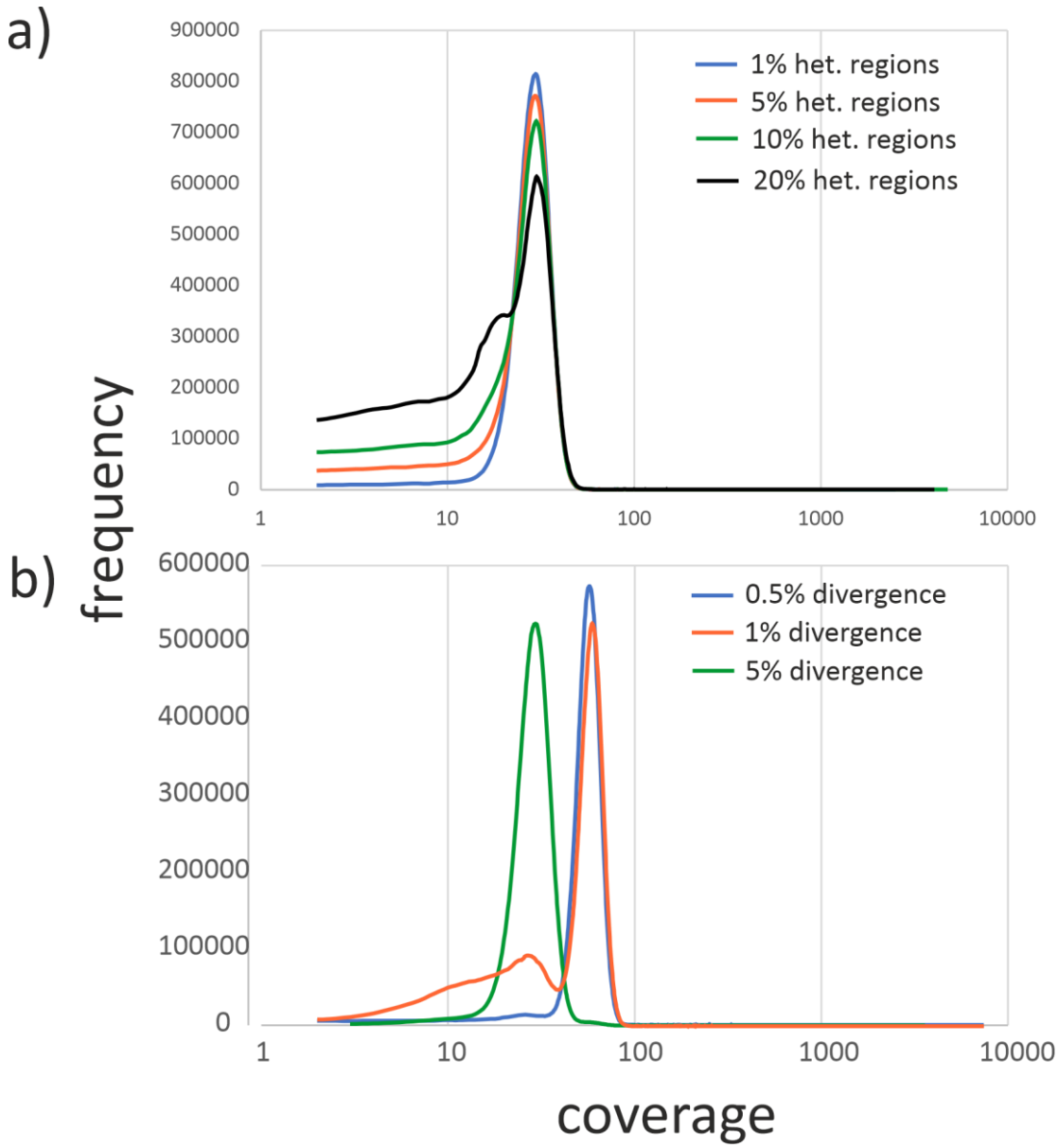

262

263 Figure 3. Coverage distributions for divergent heterozygous and tetraploid genomes. All distributions
264 shown are based on the *Saccharomyces_cerevisae*_like genome. a) Coverage distributions for 0%, 5%
265 10% and 20% of divergent heterozygous regions. b) Coverage distributions for tetrapoid genomes
266 with 0.5%, 1% and 5% divergence among the duplicated genomes. Please note the logarithmic scale
267 of the x-axes.

Empirical data

Ordinary Least Squares Regression of 1C flow-cytometry estimates against the estimates derived from the coverage approach yielded an excellent fit ($r^2 = 0.998$, $p = 2.2 \times 10^{-34}$). Removing the outlier estimate for the crayfish genome did not change the result markedly ($r^2 = 0.958$, $p = 2.1 \times 10^{-17}$). The estimated slope was with 0.996+/- 0.043 (s.e.) very close to unity. The fit of the respective k-mer based estimates to the flow cytometry data was equally good ($r^2 = 0.996$, $p = 1.1 \times 10^{-26}$), however, the slope of 0.585 +/- 0.007 (s.e.) suggested a systematically lower k-mer estimate (Figure 2). The estimated slopes were significantly different from each other ($t = 9.43$, d.f. = 44, $p < 1 \times 10^{-6}$).

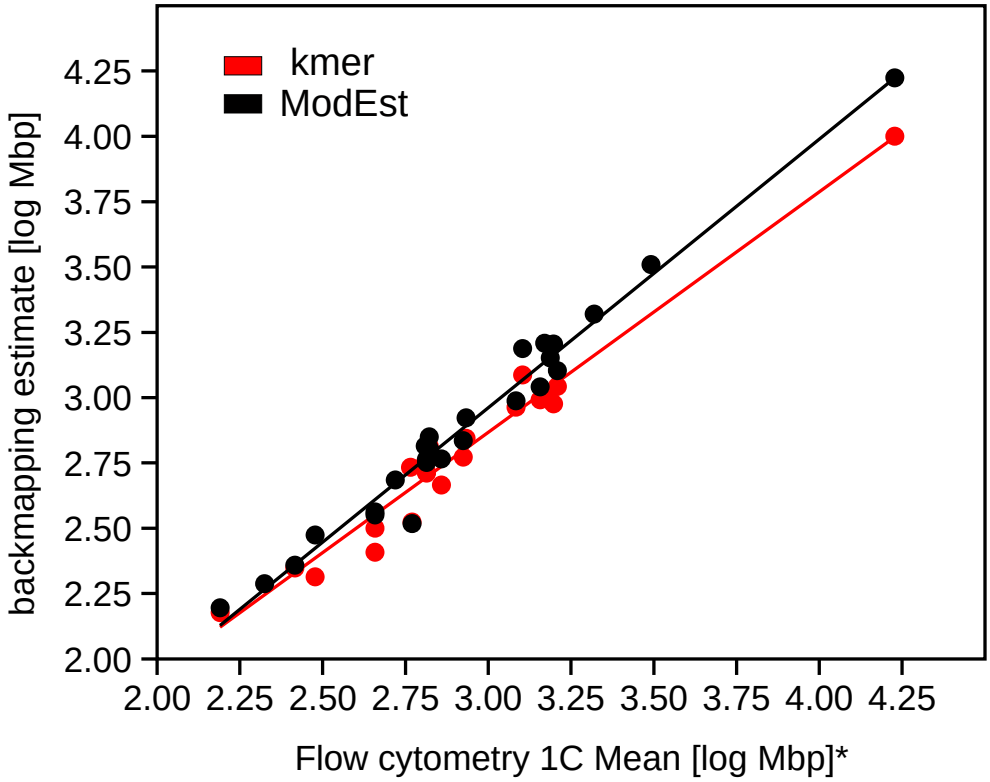

Figure 5. Ordinary least square regression for N_{bm}/m (black) and k-mer based (red) genome size estimates on 1C flow-cytometry estimates derived from the same individuals, respectively. For better graphical representation, estimates were log transformed. Both regressions were highly significant ($p < 0.0001$). The N_{bm}/m estimates fit as well ($r^2 = 0.998$) than their k-mer based counterparts ($r^2 = 0.996$). The slopes (0.995 for N_{bm}/m and 0.59 for k-mer based) were significantly different.

282 ## *Discussion*

283 As long as reliable whole chromosome sequencing is technically not yet feasible and thus the true
284 genome size is not known, genome size estimation of *de novo* sequenced genomes will be a
285 necessary and important part of biodiversity genomics. We presented here with ModEst a fast, easy-
286 to-use and precise method for genome size estimation from NGS sequencing data. We have shown
287 that the method works for a wide range of genome sizes. The method could become standard part of
288 the genome assembly process, because it relies on data that is routinely collected. Albeit our method
289 is not the first to propose the use of sequencing, respectively mapping statistics (Pflug *et al.* 2020;
290 Pucker 2019), it requires less assumptions and much less bioinformatic effort than previously
291 suggested approaches. The method does, admittedly, not solve the problem how much sequence
292 information should be produced in the first place if there is absolutely no *a priori* information on the
293 expected genome size of the target organism. However, very low modal coverages obtained with the
294 method indicate that sequencing efforts should be increased.

295 To evaluate the performance of our method and the factors influencing it, we performed a
296 simulation study. We simulated five different genomes with the characteristics and genome sizes
297 typical for various eukaryotic taxa. We could show that the precision of the estimate is largely
298 independent from the contiguity and quality of the underlying genome assembly as long as most
299 sequence elements in the genome are represented in the assembly draft. This finding was confirmed
300 with the empirical samples, where e.g. the size estimate for giant genome of the crayfish *Astacus*
301 *astacus* was gained from a very preliminary, highly discontinuous assembly with poor N50, which
302 nevertheless yielded excellent concordance with the flowcytometry estimates (Table 2). This makes
303 the method particularly suitable to obtain a reliable genome size estimate early in the assembly
304 process and, if necessary, adjust the sequencing strategy. But also genome skimming projects
305 (Dodsworth 2015) with low coverages could profit from the proposed method, as long as the
306 obtained coverage is at least in the order of 2-5X. The simulations have further shown that divergent
307 heterozygote stretches do not compromise the result of the genome size estimation.

308 The accuracy of genome size estimates of simulated tetraploid organisms depended strongly on the
309 degree of divergence between the genome copies. When the divergence was low (0.5%), the
310 assembly of the duplicated was almost completely collapsed and consequently the modal coverage
311 twice as high as the true coverage. However, already with 1% sequence divergence between the
312 duplicated genomes, an additional peak close to the true value of 30 was observed. For 5% sequence
313 divergence and higher (not shown), the assembly more or less fully resolved the duplicated genomes
314 and the highest peak was identical to the true coverage. This stressed that multimodal coverage
315 distributions point to issues with the assembly and should always be carefully investigated.

316 Nevertheless, if the ploidy of the organism is known, reliable estimates of the genome size can be
317 gained even for recent polyploidisation events with our method as well.

318 The simulation study relied on simulated short reads as obtained e.g. by the widespread Illumina-
319 platform. However, several included empirical examples (e.g. Chueca *et al.* 2021a) suggested that
320 estimating the bases sequenced from the target genome with PacBio long reads worked equally well.
321 In principle, as long as the assumption of random sequencing of bases from the genome is fulfilled,
322 every sequencing platform should yield reliable estimates. For mixed assemblies, however, it is
323 advisable to use only one sort of data (preferably the one with the higher number of sequenced
324 bases, see below), because the underlying coverage distributions are usually different.

325 We proposed four slightly different estimators of genome size. Simulations indicated that, as
326 expected, the N_{clean}/λ estimator yielded by far the best results, in practice largely independent of
327 coverage or assembly quality. However, since we gained the reads from simulated genomes, they
328 were by definition free of contaminations, i.e. reads from other organisms or other (e.g. organellar)
329 genomes. Whether $N_{clean,}$ the number of bases sequenced after cleaning and trimming, is reasonable
330 for empirical estimations depends thus on the confidence with regard to the amount of residual
331 contamination in the data set.

332 For the alternative, using the number of back-mapped reads, N_{bm}, as an estimator of the bases
333 sequenced, precision depended strongly on the completeness of the genome assembly in terms of
334 presence of all sequence elements, regardless of their copy-number. This seemed reasonable: if all
335 repeat classes and complex regions are represented in the genome draft, all reads will find a place
336 they can map to. If the confidence is high that N_{clean} is correct, the ratio N_{bm}/N_{clean} would be a good
337 indicator of genome completeness in this sense.

338 We have shown that the λ parameter of the underlying true Poisson distribution of base coverage is
339 readily and reliably found by ML estimation, if we truncate the data to a small window around the
340 modal value of the coverage distribution. Moreover, because the modal value of a Poisson
341 distribution cannot deviate more than 1 from λ, the relative error from using m instead of λ
342 decreases with increasing coverage. Most genome sequencing projects use coverages of several
343 dozen X for at least one technique where the difference becomes marginal. Estimating genome size
344 from low coverage e.g. of genome-skimming projects, however, should entail proper estimation of λ.

345 Comparison of genome size estimates obtained with our sequencing coverage method to empirical
346 data from flow cytometry obtained from the same individual achieved very good agreement,
347 regardless of genome size. The regression slope of close to 1 indicated that the estimates obtained
348 with our method can be used interchangeably with those from flow-cytometry. This allows

349 researchers to gather reliable and comparable genome size estimates for species where fresh
350 material is difficult or impossible to obtain or access to flow-cytometry equipment is lacking.

351 While the k-mer based estimates available were almost as consistent as those obtained from
352 sequencing coverage, they were not as precise. The k-mer approach consistently underestimated the
353 true size by more than one third. By their very nature, k-mer approaches estimate rather the content
354 of high complexity regions (Lipovský *et al.* 2017). It will be therefore interesting to see whether the
355 observed taxon-independent relationship of approximately 2/3 complexity regions to 1/3 repeat
356 regions as found here mainly for animal species will hold true for more genomes. The work of Novák
357 et al. (2020) also showed an almost constant, albeit higher proportion of repetitive regions for plant
358 genomes with sizes up to 10 Gb.Above this size, the relative proportion of repeats declined.
359 Obtaining more reliable genome sizes from a broad taxon range will allow to infer which processes
360 are driving these patterns to which the proposed ModEst method can contribute.

361 *Acknowledgements*

362 We thank our LOEWE-TBG colleagues for giving us early access to their assembled genomes.

363 *Data Accessibility Statement*

364 All genomes specifically simulated for this publication will be made available via Dryad.

365 *References*

366 Agudo AB, Torices R, Loureiro J, *et al.* (2019). Genome size variation in a hybridizing diploid species
367 complex in *Anacyclus* (Asteraceae: Anthemideae). *International Journal of Plant Sciences* **180**,
368 374-385.

369 Asalone KC, Ryan KM, Yamadi M*, et al.* (2020) Regional sequence expansion or collapse in
370 heterozygous genome assemblies. *PLoS Computational Biology* **16**, e1008104.

371 Bankevich A, Nurk S, Antipov D*, et al.* (2012) SPAdes: a new genome assembly algorithm and its
372 applications to single-cell sequencing. *Journal Of Computational Biology* **19**, 455-477.

373 Bennett MD, Leitch IJ (2005) Genome size evolution in plants. *The evolution of the genome*, pp. 89-
374 162. Elsevier.

375 Blommaert J, Riss S, Hecox-Lea B, *et al.* (2019) Small, but surprisingly repetitive genomes: transposon
376 expansion and not polyploidy has driven a doubling in genome size in a metazoan species
377 complex. *BMC Genomics* **20**, 466

Böhning D, Schön D (2005) Nonparametric maximum likelihood estimation of population size based on the counting distribution. *Journal of the Royal Statistical Society: Series C (Applied Statistics)* **54**, 721-737.

Bolger AM, Lohse M, Usadel B (2014) Trimmomatic: a flexible trimmer for Illumina sequence data. *Bioinformatics* **30**, 2114-2120.

Challis R, Richards E, Rajan J, *et al.* (2020) BlobToolKit – Interactive Quality Assessment of Genome Assemblies. *G3: Genes, Genomes, Genetics* **10**, 1361–1374.

Carta A, Bedini G, Peruzzi L (2020). A deep dive into the ancestral chromosome number and genome size of flowering plants. *New Phytologist* **228**, 1097-1106.

Chueca L, Kochmann J, Schell T*, et al.* (2021a) De novo Genome Assembly of the Raccoon Dog (*Nyctereutes procyonoides*). *Frontiers in Genetics* **12***: 658256. doi: 10.3389/fgene*.

Chueca LJ, Schell T, Pfenninger M (2021b) De novo genome assembly of the land snail *Candidula unifasciata* (Mollusca: Gastropoda). *G3: Genes, Genomes, Genetics* **11**, jkab180*.*

Cohen J, Cohen P, West SG, Aiken LS (2013) *Applied multiple regression/correlation analysis for the behavioral sciences* Routledge.

Danecek P, Bonfield JK, Liddle J, *et al.* (2021) Twelve years of SAMtools and BCFtools. *GigaScience* **10**, giab008, https://doi.org/10.1093/gigascience/giab008.

David F, Johnson N (1952) The truncated poisson. *Biometrics* **8**, 275-285.

Delignette-Muller ML, Dutang C (2015) fitdistrplus: An R package for fitting distributions. *Journal of Statistical Software* **64**, 1-34.

Dodsworth S (2015) Genome skimming for next-generation biodiversity analysis. *Trends in Plant Science* **20**, 525-527.

Doležel J, Greilhuber J (2010) Nuclear genome size: are we getting closer? *Cytometry Part A* **77**, 635-642.

Elliott TA, Gregory TR (2015) What's in a genome? The C-value enigma and the evolution of eukaryotic genome content. *Philosophical Transactions of the Royal Society B: Biological Sciences* **370**, 20140331.

Fountain ED, Pauli JN, Reid BN, *et al.* (2016) Finding the right coverage: the impact of coverage and sequence quality on single nucleotide polymorphism genotyping error rates. *Molecular Ecology Resources* **16**, 966-978.

408 García-Alcalde F, Okonechnikov K, Carbonell J*, et al.* (2012) Qualimap: evaluating next-generation
409 sequencing alignment data. *Bioinformatics* **28**, 2678-2679.

410 Gardner JD, Laurin M, Organ CL (2020) The relationship between genome size and metabolic rate in
411 extant vertebrates. *Philosophical Transactions of the Royal Society B* **375**, 20190146.

412 Hare EE, Johnston JS (2012) Genome size determination using flow cytometry of propidium iodide-
413 stained nuclei. In: *Molecular methods for evolutionary genetics* (pp. 3-12). Humana Press.

414 Hartke J, Schell T, Jongepier E*, et al.* (2019) Hybrid genome assembly of a neotropical mutualistic ant.
415 *Genome Biology and Evolution* **11**, 2306-2311.

416 Heckenhauer J, Frandsen PB, Gupta DK*, et al.* (2019) Annotated draft genomes of two caddisfly
417 species *Plectrocnemia conspersa* CURTIS and *Hydropsyche tenuis* NAVAS (Insecta:
418 Trichoptera). *Genome Biology and Evolution* **11**, 3445-3451.

419 Heckenhauer J, Frandsen PB, Sproul JS, *et al.* (2021) Genome size evolution in the diverse insect
420 order Trichoptera. *bioRxiv* doi: https://doi.org/10.1101/2021.05.10.443368

421 Huang W, Li L, Myers JR, Marth GT (2012) ART: a next-generation sequencing read simulator.
422 *Bioinformatics* **28**, 593-594.

423 Johnston JS, Bernardini A, Hjelmen CE (2019) Genome size estimation and quantitative cytogenetics
424 in insects. In: *Insect genomics*, pp. 15-26. Springer.

425 Kapusta A, Suh A, Feschotte C (2017). Dynamics of genome size evolution in birds and mammals.
426 *Proceedings of the National Academy of Sciences* **114**, E1460-E1469.

427 Keyl H-G (1965) A demonstrable local and geometric increase in the chromosomal DNA of
428 *Chironomus*. *Experientia* **21**, 191-193.

429 Kumar S, Jones M, Koutsovoulos G, *et al.* (2013) Blobology: exploring raw genome data for
430 contaminants, symbionts and parasites using taxon-annotated GC-coverage plots. *Frontiers*
431 *in Genetics* **4**, 237.

432 Lefébure T, Morvan C, Malard F*, et al.* (2017) Less effective selection leads to larger genomes.
433 *Genome Research* **27**, 1016-1028.

434 Li H (2013) Aligning sequence reads, clone sequences and assembly contigs with BWA-MEM. *arXiv*
435 *preprint arXiv:1303.3997*.

436 Li X, Waterman MS (2003) Estimating the repeat structure and length of DNA sequences using ℓ-
437 tuples. *Genome Research* **13**, 1916-1922.

438 Lipovský M, Vinar T, Brejova B (2017) Approximate abundance histograms and their use for genome
439 size estimation,*ITAT 2017* 27-34.

440 Lynch M, Conery JS (2003) The origins of genome complexity. *Science* **302**, 1401-1404.

441 Marçais G, Kingsford C (2011) A fast, lock-free approach for efficient parallel counting of occurrences
442 of k-mers. *Bioinformatics* **27**, 764-770.

443 Mishra B, Ploch S, Runge F*, et al.* (2020) The genome of *Microthlaspi erraticum* (Brassicaceae)
444 provides insights into the adaptation to highly calcareous soils. *Frontiers in Plant Science* **11**,
445 943.

446 Mishra B, Ulaszewski B, Meger J*, et al.* (2021) A chromosome-level genome assembly of the
447 European Beech (*Fagus sylvatica*) reveals anomalies for organelle DNA integration, repeat
448 content and distribution of SNPs. *bioRxiv 2021.03.22.436437*.

449 Nadarajah S, Kotz S (2006) R programs for computing truncated distributions. *Journal of Statistical*
450 *Software*, ***16,*** *Code Snippet 2.*

451 Nickel JH, Schell T, Holtzem T*, et al.* (2021) Hybridization dynamics and extensive introgression in the
452 *Daphnia longispina* species complex: new insights from a high-quality *Daphnia galeata*
453 reference genome. *bioRxiv 2021.02.01.429177*.

454 Novák P, Guignard MS, Neumann P, *et al.* (2020). Repeat-sequence turnover shifts fundamentally in
455 species with large genomes. *Nature Plants* **6**, 1325-1329.

456 Oliver MJ, Petrov D, Ackerly D, *et al.* (2007) The mode and tempo of genome size evolution in
457 eukaryotes. *Genome Research* **17**, 594-601.

458 Petrov DA (2001) Evolution of genome size: new approaches to an old problem. *Trends in Genetics*
459 **17**, 23-28.

460 Pflug JM, Holmes VR, Burrus C, *et al.* (2020) Measuring genome sizes using read-depth, k-mers, and
461 flow cytometry: methodological comparisons in beetles (Coleoptera). *G3: Genes, Genomes,*
462 *Genetics* **10**, 3047-3060.

463 Poptsova MS, Il'Icheva IA, Nechipurenko DY, *et al.* (2014). Non-random DNA fragmentation in next-
464 generation sequencing. *Scientific Reports* **4**, 1-6.

465 Prokopowich CD, Gregory TR, Crease TJ (2003) The correlation between rDNA copy number and
466 genome size in eukaryotes. *Genome* **46**, 48-50.

467 Pucker B (2019) Mapping-based genome size estimation. *bioRxiv* https://doi.org/10.1101/607390

468 Quinlan AR, Hall IM (2010) BEDTools: a flexible suite of utilities for comparing genomic features.
469 *Bioinformatics* **26**, 841–842.

470 Schell T, Feldmeyer B, Schmidt H*, et al.* (2017) An annotated draft genome for *Radix auricularia*
471 (Gastropoda, Mollusca). *Genome Biology and Evolution* **9**, 585-592.

472 Sims D, Sudbery I, Ilott NE, Heger A, *et al.* (2014) Sequencing depth and coverage: key considerations
473 in genomic analyses. *Nature Reviews Genetics* **15**, 121-132.

474 Sohn J-i, Nam J-W (2018) The present and future of de novo whole-genome assembly. *Briefings in*
475 *Bioinformatics* **19**, 23-40.

476 Treangen TJ, Salzberg SL (2012) Repetitive DNA and next-generation sequencing: computational
477 challenges and solutions. *Nature Reviews Genetics* **13**, 36-46.

478 Vitales D, Álvarez I, Garcia S, *et al.* (2020). Genome size variation at constant chromosome number is
479 not correlated with repetitive DNA dynamism in *Anacyclus* (Asteraceae). *Annals of Botany*
480 **125**, 611-623.

481 Vurture GW, Sedlazeck FJ, Nattestad M*, et al.* (2017) GenomeScope: fast reference-free genome
482 profiling from short reads. *Bioinformatics* **33**, 2202-2204.

483 Wang J, Liu J, Kang M (2015) Quantitative testing of the methodology for genome size estimation in
484 plants using flow cytometry: a case study of the *Primulina* genus. *Frontiers in Plant Science* **6**,
485 354.

486 Winter S, Prost S, De Raad J*, et al.* (2020) Chromosome-level genome assembly of a benthic
487 associated Syngnathiformes species: the common dragonet, *Callionymus lyra*. *Gigabyte* **1***,*
488 *https://doi.org/10.46471/gigabyte.6*

489

490

Supplement

R-code for estimating lambda from a truncated Poisson distribution

```
library(fitdistrplus)
library(truncdist)
library(splitstackshape)
#transform Qualimap output to R-object
obj <- read.table("coverage_histogram.txt", header = TRUE)
obj <- expandRows(obj, "freq")
obj <- as.vector(obj$freq)
summary(obj)
#define function for mode
mode <- function(obj) {uniqv <- unique(obj) uniqv[which.max(tabulate(match(obj, uniqv)))]}
min <- mode – 5
max <- mode + 5
dtruncated_poisson <- function(x, lambda) {dtrunc(x, "pois", a=min, b=max, lambda=lambda)}
ptruncated_poisson <- function(q, lambda) {ptrunc(q, "pois", a=min, b=max, lambda=lambda)}
fitdist(obj, "pois", start = list(lambda = mode))
```

508 Supplemental Table 1. Genome size estimates and deviations from true value for the simulated genomes.

simulated genome	coverage	estimated λ	modal coverage m	N_{clean}/λ	deviation N_{clean}/λ	N_{clean}/m	deviation N_{clean}/m	N_{bm}/λ	deviation N_{bm}/λ	N_{bm}/m	N_{bm}/m
Saccharomyces_cerevisae_like	10X	9.995	9	12.08	-0.00044	13.42	0.11109	11.30	-0.06500	12.56	0.03933
	30X	29.994	29	12.08	-0.00015	12.50	0.03446	11.30	-0.06447	11.69	-0.03209
	60X	59.998	59	12.08	-0.00003	12.29	0.01693	11.29	-0.06505	11.49	-0.04920
Caenorhabditis_elegans_like	10X	9.996	9	100.04	-0.00010	111.15	0.11103	93.37	-0.06678	103.74	0.03694
	30X	29.995	29	100.03	-0.00019	103.49	0.03441	93.56	-0.06487	96.79	-0.03251
	60X	59.994	59	100.04	-0.00003	101.73	0.01688	93.31	-0.06736	94.88	-0.05159
Arabidopsis_thaliana_like	10X	9.993	9	120.04	-0.00038	133.42	0.11102	95.63	-0.20365	106.29	-0.11490
	30X	29.996	29	120.07	-0.00016	124.22	0.03440	96.02	-0.20037	99.34	-0.17273
	60X	59.992	59	120.08	-0.00005	122.11	0.01687	95.98	-0.20075	97.60	-0.18723
Drosophila_melanogaster_like	10X	9.998	9	143.98	-0.00056	160.06	0.11100	111.75	-0.22432	124.22	-0.13773
	30X	29.992	29	144.05	-0.00009	149.02	0.03438	112.72	-0.21756	116.61	-0.19059
	60X	59.988	59	144.06	-0.00003	146.49	0.01685	112.09	-0.22198	113.98	-0.20884
Scophthalmus_maximus_like	10X	9.996	9	523.93	-0.00027	582.29	0.11110	521.90	-0.00414	580.04	0.10680
	30X	29.995	29	524.05	-0.00004	542.13	0.03448	522.34	-0.00330	540.37	0.03111
	60X	59.998	59	524.03	-0.00008	532.95	0.01694	522.27	-0.00344	531.16	0.01353
Saccharomyces_cerevisae_like 1% divergent heterozygous regions	30X	29.999	30	11.87	-0,01747	11.87	-0,01749	11.74	-0,02827	11.74	-0,02829

5% divergent heterozygous regions	30X	29.999	30	11.80	-0,02321	11.80	-0,02324	11.68	-0,03286	11.68	-0,03288
10% divergent heterozygous regions	30X	29.999	30	11.71	-0,03038	11.71	-0,03040	11.57	-0,04228	11.57	-0,04230
20% divergent heterozygous regions	30X	29.999	30	11.54	-0,04504	11.54	-0,04507	11.40	-0,05666	11.40	-0,05668
Tetraploid Saccharomyces_cerevisae_like 0.5% divergence among duplicated genomes	30X	59.999	59	11.88	-0.50819	12.08	-0.49986	11.67	-0.51685	11.87	-0.50867
1% divergence	30X	59.988	59	11.89	-0.50804	12.08	-0.49980	11.62	-0.51924	11.81	-0.51119
1% divergence, correct peak	30X	28.986	28	24.60	0.01815	25.46	0.05398	24.04	-0.00502	24.88	0.03000
5% divergence	30X	29.999	29	23.81	-0.01431	24.63	0.01965	23.34	-0.03376	24.15	0.00047

509